COUPLING BETWEEN THE BACTERIORHODOPSIN PHOTOCYCLE AND THE PROTONMOTIVE FORCE IN *HALOBACTERIUM HALOBIUM* CELL ENVELOPE VESICLES

III. Time-resolved Increase in the Transmembrane Electric Potential and Modeling of the Associated Ion Fluxes

S. L. HELGERSON, M. K. MATHEW, D. B. BIVIN, P. K. WOLBER, E. HEINZ,* AND W. STOECKENIUS

*Department of Biochemistry and Biophysics and Cardiovascular Research Institute, University of California, San Francisco, California 94143; and *Department of Physiology, Cornell University Medical College, New York, New York 10021*

ABSTRACT Bacteriorhodopsin functions as an electrogenic, light-driven proton pump in *Halobacterium halobium*. In cell envelope vesicles, its photocycle kinetics can be correlated with membrane potential. The initial decay rate of the M photocycle intermediate(s) decreases with increasing membrane potential, allowing the construction of a calibration curve. The laser (592.5 nm) was flashed at various time delays following the start of background illumination (592 ± 25 nm) and transient absorbance changes at 418 nm monitored in cell envelope vesicles. The vesicles were loaded with and suspended in either 3 M NaCl or 3 M KCl buffered with 50 mM HEPES at pH 7.5 and the membrane permeability to protons modified by pretreatment with *N,N'*-dicyclohexylcarbodiimide. In each case the membrane potential rose with a halftime of ~75 ms. The steady-state potential achieved depends on the cation present and the proton permeability of the membrane, i.e., higher potentials are developed in dicyclohexylcarbodiimide treated vesicles or in NaCl media as compared with KCl media. The results are modeled using an irreversible thermodynamics formulation, which assumes a constant driving reaction affinity (A_{ch}) and a variable reaction rate (J_r) for the proton-pumping cycle of bacteriorhodopsin. Additionally, the model includes a voltage-gated, electrogenic Na^+/H^+ antiporter that is active when vesicles are suspended in NaCl. Estimates for the linear phenomenological coefficients describing the overall proton-pumping cycle ($L_r = 3.5 \times 10^{-11}$/mol^2/J · g · s), passive cation permeabilities ($L^u_H = 2 \times 10^{-10}$, $L^u_K = 2.2 \times 10^{-10}$, $L^u_{Na} = 1 \times 10^{-11}$), and the Na^+/H^+ exchange via the antiporter ($L_{ex} = 5 \times 10^{-11}$) have been obtained.

INTRODUCTION

Bacteriorhodopsin (bR) is the best established example of an electrogenic, proton pump as postulated in the chemiosmotic theory of energy coupling (Mitchell, 1968). The distinct crystalline structure of purple membrane largely precludes any direct interaction of the proton pump with the driven processes, e.g., ATP synthesis, ion transport, and amino acid transport (for reviews see Stoeckenius et al., 1979; Stoeckenius and Bogomolni, 1982). Other proposed energy-coupling mechanisms that postulate more direct interactions between the primary and secondary energy converters are largely precluded in this system (Westerhoff et al., 1984). However, a detailed understanding of the electrogenic pumping cycle of bR is necessary to define possible modes of energy coupling. Also, the transmembrane transport of protons has previously been related mostly to the generation of a pH gradient, i.e., to the chemical part of the protonmotive force. Its direct contribution to the electric component of the protonmotive force has in our opinion not yet been sufficiently considered. To quantitatively define the coupling of proton pumping by bR to the driven processes we are examining in vivo (*a*) the coupling between the bR photocycle and the generated protonmotive force (Dancshazy et al., 1983; Groma et al., 1984) and (*b*) the coupling between the protonmotive force and ATP synthesis (Helgerson et al., 1983). Our goal is to develop both the experimental and theoretical techniques needed to mathematically model energy coupling in *Halobacterium halobium* (*H. halobium*).

The research reported here addresses two outstanding

Dr. Wolber's current address is Advanced Genetic Sciences, Inc., 6701 San Pablo Avenue, Oakland, CA 94608.

Dr. Heinz's current address is Max-Planck-Institut für Ernährungsphysiologie, D-4600 Dortmund 1, Federal Republic of Germany.

problems in bioenergetics. Experimentally, an accurate well-defined probe is needed to quantitate the development and magnitude of the protonmotive force in small vesicles and intact cells. Theoretically, testable equations are required to describe both the probe's response mechanism and the coupled ion flows and driven systems being monitored. Heinz (1980, 1982) has proposed a model using the theory of irreversible processes that we have now tested and extended to provide the necessary theoretical formalism. The experiments performed to test this model use bR as an intrinsic membrane-bound probe to monitor the delocalized transmembrane protonmotive force in *H. halobium*. The ability of a single energy-converting protein to both generate and monitor the protonmotive force provides a unique and powerful method to test bioenergetic mechanisms in intact biological systems.

GLOSSARY

Source of Chemicals and Abbreviations

Sigma Chemical Co. (St. Louis, MO): cesium chloride, deoxyribonuclease; N-2-hydroxyethylpiperazine-N'-2-ethane sulfonic acid (HEPES); 2-methyl-1,4-napthoquinone (menadione); nicotine adenine dinucleotide (reduced form); Tris-hydroxymethylaminomethane. Pharmacia Fine Chemicals (Piscataway, NJ): Ficoll 400. Pierce Chemical Co. (Rockford, IL): *N,N'*-dicyclohexylcarbodiimide (DCCD). New England Nuclear (Boston, MA): (^{14}C)-sucrose (39 mCi mmol^{-1}); triphenylmethylphosphonium bromide (1.13 Ci mmol^{-1}) (^{3}H-TPMP^{+}); $^{3}H_2O$ (1 mCi g^{-1}).

List of Symbols

M_1, M_2	pre-exponential (initial concentration) factors of the exponential decays describing the fast and slow M photointermediates
k_1, k_2	decay rate of the corresponding M form
f	branching ratio giving the fraction of bR molecules photocycling through M_1
f_c	constant defining the dependence of log (f) on $\Delta\Psi$
$\Delta\Psi$	membrane electric potential
ΔpIon	concentration gradient of given ion
X_i	osmotic driving force of given ion
A_{ch}	effective affinity of the electrogenic bR-protonpumping cycle (assumed constant)
J_r	rate of the bR pumping cycle (assumed variable)
L_r	phenomenological coefficient for the bR pumping cycle
J_{ion}	net flow of given ion; outward ion movements are defined as the negative direction
L^u_{ion}	phenomenological leakage coefficient for the given ion
L_{ex}	phenomenological coefficient for ion exchange through the protonmotive force-gated Na^+/H^+ antiporter
ν^{ion}	stoichiometric coefficient for the given ion in a coupled process
$n_{ex}(t)$	fraction of the Na^+/H^+ antiporter population active at any time after the membrane potential exceeds the gating potential
B	buffering capacity of the medium for a given ion
C	electrical capacity of the membrane
F	Faraday constant
R	gas constant
T	temperature
t	time.

MATERIALS AND METHODS

Preparation of Cell Envelope Vesicles

Envelope vesicles of *H. halobium* strain JW-3 were prepared as described previously (Groma et al., 1984) except that a continuous linear density gradient was used: Ficoll (4.5%) dissolved in NaCl (4 to 3.65 M) and CsCl (0 to 0.45 M) with ρ = 1.162 to 1.205 on a cushion of Ficoll (22.5%)/NaCl(4 M) ρ = 1.212. The vesicles banded between ρ = 1.170 and 1.185 while the nonvesicular fraction was stopped by the cushion layer. Protein was estimated using the Lowry assay. Orientation and intactness of the vesicle preparation were measured using the menadione reductase assay before and after lysis with Triton X-100 (Lanyi, 1972). The vesicles were loaded by osmotic shock and resuspended in 3 M NaCl or KCl containing 50 mM HEPES (pH 7.5). Vesicles prepared in this manner were >90% intact and oriented right-side out. Where indicated the vesicles (9 mg protein/ml) in buffered NaCl or KCl were preincubated with 25 μM DCCD at 0°C for 24 h (Michel and Oesterhelt 1980); washed once and resuspended in the same medium without DCCD. The transmembrane electric potential was measured using the flow dialysis assay of (^{3}H)-triphenylmethylphosphonium uptake (Lanyi et al., 1979; Groma et al., 1984].

Time-resolved Absorbance Changes

We used an instrument similar to that described previously (Dancshazy et al., 1983; Groma et al., 1984). The transient absorbance changes of vesicle samples in a 3 × 3 mm cuvette were measured using a 418 nm monitoring beam (100 W tungsten lamp and a H-20 monochromator; Instruments, SA Inc., J-Y Optical Systems Div., Metuchen, NJ) and a Hamamatsu R928 photomultiplier tube (Hamamatsu Corp.; Middlesex, NJ). The photomultiplier tube was protected by a Corning 1-60 didymium glass filter (Corning Glass Works, Corning, NY) and a 418 nm interference filter (Baird-Atomic, Inc., Bedford, MA). Actinic illumina-

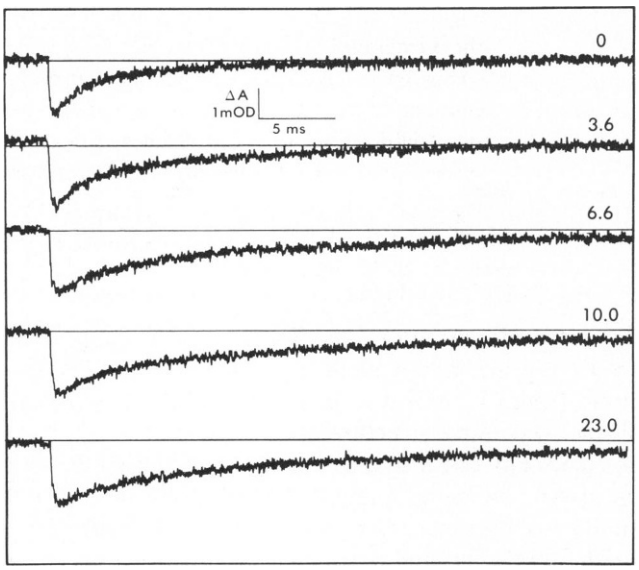

FIGURE 1 Laser flash-induced absorbance changes of bacteriorhodopsin at 418 nm in *H. halobium* cell envelope vesicles. The vesicles were loaded and suspended in 3 M NaCl + 50 mM HEPES (pH 7.5) at 20°C. The intensity of the continuous background illumination, in mW/cm^2, is indicated with the individual traces. The traces were acquired using 30 μs rise time on the current amplifier, which amplified the photomultiplier tube output. They are thus noisier than those presented earlier (Groma et al., 1984), which were acquired with a 300-μs rise time. Note that positive ΔA's are shown as downward displacements.

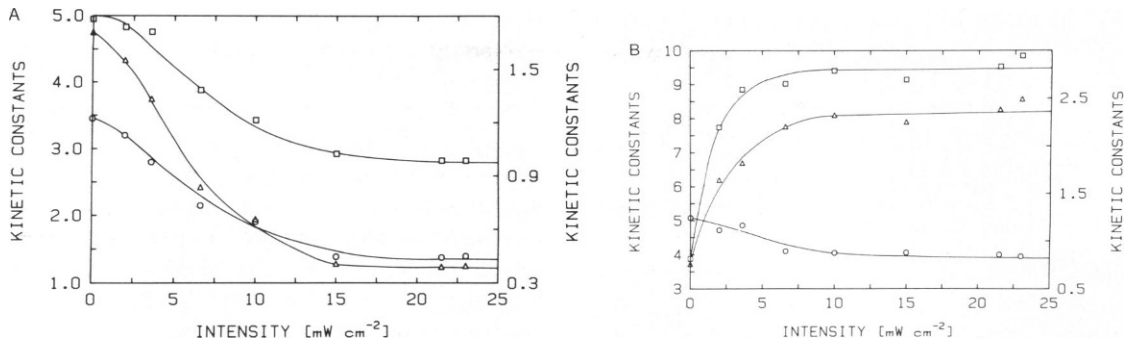

FIGURE 2 Kinetic constants, amplitudes (M), and decay constants (k), of two exponentials fitted to the data of absorbance changes obtained under steady illumination as in Fig. 1. The parameters are estimated to be accurate within 5%. (A) Parameters for the fast component (○) $M_1 \times 10^4$ OD: (□) $k_1 \times 10^{-2}$ s^{-1}, both using left-hand scale; (△) M_1k_1 OD s^{-1}, using the right-hand scale. (B) Parameters for the slow component. (△) $M_2 \times 10^4$ OD using the right-hand scale; (○) $k_2 \times 10^{-1}$ s^{-1}, (□) $M_2k_2 \times 10^2$ OD s^{-1}, both using the left-hand scale.

tion was provided at a right angle to the monitoring beam through a bifurcated light pipe. Light from a 150 W arc lamp was focused on one light pipe input after heat filtering and passage through a Corning 3-66 glass filter (50% transmittance at 575 nm; Corning Glass Works) plus a Corion BB5920CC interference filter (592 ± 25 nm halfband width; Corion Corp., Holliston, MA). Illumination intensity was controlled with neutral density filters and the duration was varied using a solenoid-activated shutter and a Grass Instruments S-44 pulse generator (Grass Instrument Co., Quincy, MA). Actinic laser pulses (dye laser, 592.5 nm, 7 ns; Molectron Corp., Sunnyvale, CA) entered the light pipe through the other input.

The sample was illuminated with light from the arc lamp in cycles of 1 s ON and 4 s OFF. A laser pulse was delivered at various times in this cycle and the transient changes in the photomultiplier output amplified using a current amplifier with a 30 μs rise time (model 427; Keithley Instruments, Cleveland, OH). 64 transients were averaged and stored using a Nicolet 1180 computer system (4K points, 10 μs/point; Nicolet Instrument Corp., Madison, WI). A similar data set was collected without the laser pulse. This monitored transmission changes due to the buildup of photocycle intermediates induced by the background illumination. The latter data set was subtracted from the former and the difference converted to absorbance changes for further analysis. The time-resolved data were fitted with either (*a*) one exponential rise and two decays over the entire recorded trace to obtain the amplitude and rate constants of the M_1 and M_2 components described previously (Groma et al., 1984) or (*b*) a linear decay over the first 2 ms to obtain the initial decay slope of the 418 nm absorbance changes (see Results). Both fitting programs were written in FORTRAN and run on the Nicolet 1180 computer (Nicolet Instrument Corp.).

RESULTS

Measurement of the Time-resolved Increase in the Transmembrane Electric Potential

Suspensions of *H. halobium* cells or envelope vesicle preparations show a transient absorbance change at 418 nm after a 592-nm laser light flash. This is due to the formation and decay of the bR photocycle intermediate M. The decay of M slows down when a continuous background illumination is added (Fig. 1). The background illumination generates a membrane potential by driving proton ejection from the cells or vesicles during the bR photocycle. Over the range 0–15 mWcm^{-2} the photo steady-state membrane potential is linearly dependent on light intensity (Renthal and Lanyi 1976; Groma et al., 1984). We have previously proposed that the observed biphasic kinetics of the M decay can be attributed to two spectroscopically similar M intermediates, which decay at different rates (Groma et al., 1984). The amplitudes of the two M forms

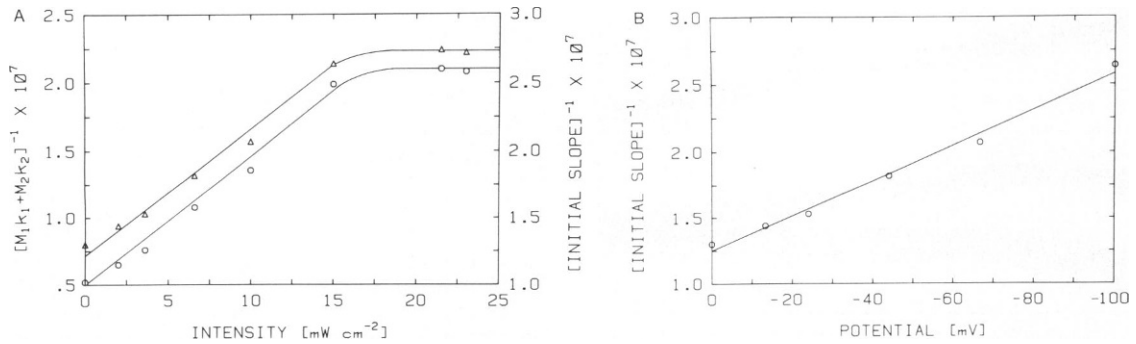

FIGURE 3 (A) Variation of the initial rate of decay of the absorbance transient at 418 nm with steady-state illumination intensity. (○) The quantity $(M_1k_1 + M_2k_2)^{-1}$ was obtained by fitting the decay to two exponentials. (△) (initial slope)$^{-1}$ obtained from a linear fit to the initial 2 ms of the decay. (B) Variation of the initial slope of the decay of the laser-induced absorbance transient at 418 nm with membrane potential in the steady state.

(M_1 and M_2) and their rate constants (k_1 and k_2) show a complex dependence on the background light intensity, i.e., membrane potential (Fig. 2 *A*, *B*). However, the reciprocal initial rate of the total M decay, $(M_1k_1 + M_2k_2)^{-1}$, is linearly related to the membrane potential (Fig. 3). We can thus use the initial rate of the flash-induced absorbance decay at 418 nm to monitor the membrane potential.

It is impractical to use kinetic constants deconvoluted from data taken over 40 ms to determine the initial decay rate and estimate the potential. Instead the linear slope of a decay curve over the first 2 ms can be used. The measured initial slopes closely follow the calculated initial rates (Fig. 3 *A*) and linearly correlate with the steady-state membrane potential (Fig. 3 *B*). This calibration curve constructed for vesicles in 3 M NaCl + 50 mM HEPES (pH 7.5) is assumed to hold in 3 M KCl + 50 mM HEPES (pH 7.5) and for vesicles pretreated with 25 μM DCCD in either medium. The kinetics of the bR photocycle are known to be sensitive to ionic strength (Kuschmitz and Hess, 1981; Mathew, M. K., and S. L. Helgerson, unpublished results). However, no significant differences in bR photocycle kinetics per se have been reported for a given high concentration of NaCl as compared with KCl. While reaction with millimolar concentrations of DCCD can perturb the bR photocycle (Jap and Glaeser, 1983), the micromolar concentrations used in this study do not. At this concentration DCCD does inhibit photophosphorylation in intact *H. halobium* cells (Michel and Oesterhelt 1980; Helgerson et al., 1983). Cell envelope vesicles do not photophosphorylate, presumably due to inactivation of the H^+/ATPase during preparation. The vesicles are leaky to protons and this leak is reduced by the DCCD treatment (Eisenbach et al., 1977).

Fig. 4 illustrates the procedure for determining the membrane potential from laser-induced absorbance transients at 418 nm. 64 transients were averaged (*C*) following laser flashes introduced with set time delays after turning on the background illumination. *A* shows the photo steady-state accumulation of M caused by the background illumination pulse. Since the baseline absorbance may change rapidly during the 40 ms period when transients are recorded, a background trace in the absence of the laser flash was recorded (*B*) and subtracted from the transient observed in the presence of the laser (*C*). The resultant data are shown in *D*. From the initial linear slope of this resulting trace the membrane potential at the time of the laser flash was determined using the calibration curve (Fig. 3 *B*). The $\Delta\Psi$ values above -100 mV were estimated using an extrapolation of the calibration curve.

In all cases tested, the membrane potential rises sharply with a $\tau_{1/2}$ of ~75 ms (Fig. 5). When the background illumination is turned off, the potential decays rapidly with a $\tau_{1/2}$ of ~25 ms. The steady-state potential achieved depends on the ionic composition of the medium (Lanyi et al., 1979) and whether or not the vesicles have been pretreated with DCCD. The lower the permeability of the vesicle membrane to the salt cation present and/or to protons, the higher the steady-state potential. The uncoupler carbonylcyanide-*m*-chlorophenylhydrazone completely prevents the development of $\Delta\Psi$ measured either by this technique or in the steady state by (^{3}H)-$TPMP^+$ uptake (data not shown).

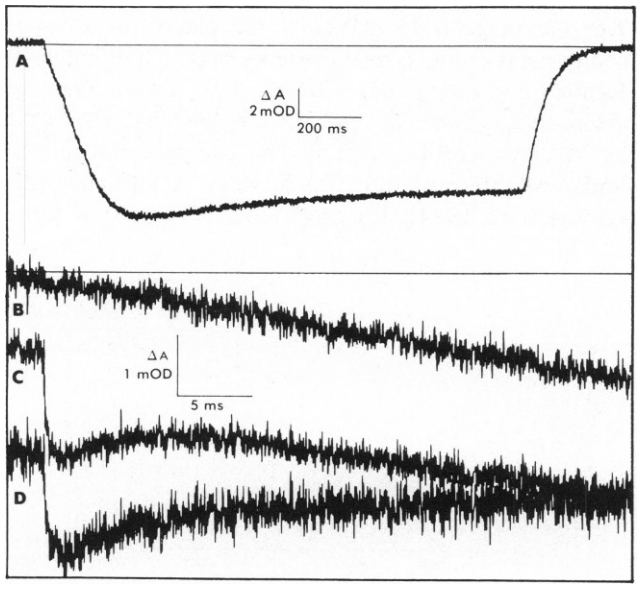

FIGURE 4 Absorbance changes at 418 nm of vesicles suspended in 3 M NaCl + 50 mM HEPES (pH 7.5). (*A*) Background illumination of 15 $mWcm^{-2}$ was turned on at first arrow and off at second. (*B–D*) The laser is flashed 75 ms after turning on background illumination. (*B*) Laser blocked; (*C*) laser unblocked; (*D*) difference between *B* and *C* for laser-induced change in absorbance.

Modeling of the Time-resolved Increase in the Transmembrane Electric Potential

Heinz (1980, 1982) has derived the kinetic equations for the development of the protonmotive force (pmf)

$$X_H = -\Delta\tilde{\mu}_{H^+} = 2.3RT\Delta pH - F\Delta\Psi \qquad (1)$$

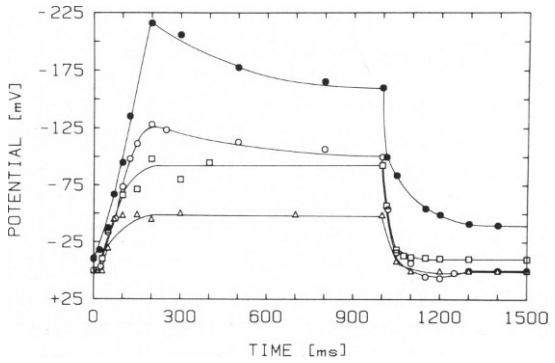

FIGURE 5 Variation in membrane potential in response to a background illumination of 15 $mWcm^{-2}$. Light is turned on at time 0 and off at 1,000 ms. Vesicles were buffered with 50 mM HEPES (pH 7.5) and suspended in 3M KCl (△); 3 M NaCl (○), both without pretreatment with DCCD; 3 M KCl (□), 3 M NaCl (●), both after DCCD pretreatment. The curves shown are visual fits to the data.

in terms of the thermodynamics of irreversible processes. An arbitrary model of a pump operating to electrogenically extrude protons from a vesicle system was analyzed. This treatment predicted that initiation of proton pumping should rapidly generate $\Delta\Psi$ in <100 ms, reaching a maximum value determined by the leakage of cations across the membrane. Due to the slow leakage of other ions a chemical gradient of protons would develop much more slowly, causing $\Delta\Psi$ to decrease but the total pmf to remain constant. Most importantly, a constant effective affinity of the pumping reaction cycle (A_{ch}), i.e., a constant driving force, was assumed such that the rate of the electrogenic pumping cycle (J_r) would decrease with increasing $\Delta\Psi$. This is in contrast to the analysis of Mitchell (1968), which assumed a constant pumping rate. The latter treatment predicts a much lower initial rise in $\Delta\Psi$ and a slower development of pmf. Here we analyze the time-resolved increase of $\Delta\Psi$ in cell envelope vesicles assuming a constant driving force. First the basic equations must be modified to account for physiological ion fluxes mediated by components in the *H. halobium* membrane.

For the development of $\Delta\Psi$ we use the equation

$$F\Delta\Psi = -A_2(e^{-\lambda_1 t} - e^{-\lambda_2 t}), \tag{2}$$

which includes the decrease in $\Delta\Psi$ concomitant with the slower development of ΔpH. For *H. halobium* cell envelope vesicles in either 3 M NaCl or KCl no significant steady-state ΔpH is formed at pH 7.5 (Lanyi et al., 1979). The buffering capacity, B, is very high, especially higher than the electric capacity, C, so that we can assume

$$-\lambda_2 \gg -\lambda_1. \tag{3}$$

Since λ_1 and λ_2 are inversely proportional to B and C, respectively, $\exp(-\lambda_1 t)$ will still be close to zero when $\exp(-\lambda_2 t)$ approaches its maximum value. During the first few hundred milliseconds after the pump has been turned on, the rise in $\Delta\Psi$ can be described by

$$F\Delta\Psi = -A_2(1 - e^{-\lambda_2 t}). \tag{4}$$

The coefficients A_2 and λ_2 for vesicles suspended in 3 M KCl or NaCl are derived as follows, with the basic assumptions that (*a*) the permeability of the membrane to ions other than H^+ and Na^+ or K^+ is negligible; (*b*) the buffering capacities for H^+, Na^+, and K^+ both inside and outside the vesicles are high enough to prevent formation of appreciable concentration gradients of these ions during the 1 s illumination period and (*c*) the only actively transported ions are ν_r^H protons per cycle of bacteriorhodopsin and an electrogenic exchange of ν_{ex}^H protons per ν_{ex}^{Na} sodium ions by the Na^+/H^+ antiporter (Lanyi and MacDonald, 1976; Eisenbach et al., 1977). ν is the stoichiometric coefficient for a given process.

For vesicles suspended in KCl

$$F\frac{d\Psi}{dt} = \frac{J_H + J_K}{C}, \tag{5a}$$

where J_H and J_K are the net flows of H^+ and K^+, respectively. Ion movements out of the vesicle are defined as the negative direction.

As discussed previously (Heinz, 1982)

$$J_H = (\nu_r^2 L_r + L_H^u)X_H - \nu_r L_r A_{ch} \tag{5b}$$

$$J_K = L_K^u X_K, \tag{5c}$$

where L_r is the phenomenological coefficient linking J_r to the driving force of the pumping cycle, ν_r^H is the proton stoichiometry of the pump, and L_H^u and L_K^u are the passive leakage coefficients for H^+ and K^+, respectively, and

$$X_H = RT\Delta pH - F\Delta\Psi \tag{5d}$$

$$X_K = RT\Delta pK - F\Delta\Psi. \tag{5e}$$

If the concentration gradients ΔpH and ΔpK are assumed to be negligible, it follows from substituting Eqs. 5b–e into Eq. 5a that

$$\frac{F d\Psi}{(\nu_r^2 L_r + L_H^u + L_K^u)F\Delta\Psi + \nu_r L_r A_{ch}} = -\frac{dt}{C} \tag{5f}$$

and by integration (Mitchell, 1968; Heinz, 1982)

$$F\Delta\Psi = -\frac{\nu_r L_r A_{ch}}{\nu_r^2 L_r + L_H^u + L_K^u}\left[1 - \exp\left(-\frac{\nu_r^2 L_r + L_H^u + L_K^u}{C}t\right)\right]. \tag{6}$$

For vesicles suspended in NaCl

$$F\frac{d\Psi}{dt} = \frac{J_H + J_{Na}}{C}. \tag{7a}$$

The net flow of protons is

$$J_H = \nu_r J_r + J_H^u + \nu_{ex}^H J_{ex}. \tag{7b}$$

The first and second terms on the right lead to the result analogous to that given in Eq. 5b. The third term describes the component of the proton flow (J_{ex}^H) through the sodium/proton antiporter

$$J_{ex}^H = \nu_{ex}^H J_{ex} = (\nu_{ex}^H)^2 L_{ex} X_H - \nu_{ex}^H \nu_{ex}^{Na} L_{ex} X_{Na}, \tag{7c}$$

where ν_{ex}^H and ν_{ex}^{Na} are the stoichiometries of proton for sodium exchange per antiporter cycle, respectively. L_{ex} is the rate coefficient that links the antiporter flow (J_{ex}) to its driving force, i.e.,

$$J_{ex} = \nu_{ex}^H L_{ex} X_H - \nu_{ex}^{Na} L_{ex} X_{Na}. \tag{7d}$$

The net flow of sodium is

$$J_{Na} = L_{Na}^u X_{Na} + \nu_{ex}^{Na} J_{ex} \tag{7e}$$

so

$$J_{Na} = L_{Na}^u X_{Na} + \nu_{ex}^{Na}\nu_{ex}^H L_{ex} X_H - (\nu_{ex}^{Na})^2 L_{ex} X_{Na}. \tag{7f}$$

Assuming as above that the concentration gradients of cations are zero, substitution of Eqs. 7b–f into Eq. 7a

gives

$$\frac{F\mathrm{d}\Psi}{\{\nu_r^2 L_r + L_H^u + L_{Na}^u + [(\nu_{ex}^H)^2 - (\nu_{ex}^{Na})^2]L_{ex}\}F\Delta\Psi + \nu_r L_r A_{ch}} = -\frac{\mathrm{d}t}{C} \quad (7g)$$

and by integration

$$F\Delta\Psi = -\frac{\nu_r L_r A_{ch}}{\nu_r^2 L_r + L_{Na}^u + L_H^u + [(\nu_{ex}^H)^2 - (\nu_{ex}^{Na})^2]L_{ex}} \cdot \left(1 - \exp\left\{-\frac{\nu_r^2 L_r + L_{Na}^u + L_H^u + [(\nu_{ex}^H)^2 - (\nu_{ex}^{Na})^2]L_{ex}}{C} t\right\}\right). \quad (8)$$

This equation differs from Eq. 6 for vesicles in KCl only by the term

$$[(\nu_{ex}^H)^2 - (\nu_{ex}^{Na})^2]L_{ex}.$$

Empirical Modifications to the Derived Membrane Potential Equations

Using Eqs. 6 or 8 the membrane potential $\Delta\Psi$ can be determined as a function of time (Fig. 7) and compared with the experimental results shown in Fig. 5. The electrical capacity of the membrane will be taken as that given by Mitchell (1968), $C = 2.2 \times 10^{-11}$ mol^2 (J · g)$^{-1}$. F is the Faraday constant equal to 9.65×10^4 J(V · mol)$^{-1}$. Preliminary estimates for the coefficients A_{ch}, ν_r^H, and the various L's were made based on published data (see Appendix).

Any individual curve shown in Fig. 5 could probably be fit using Eq. 6 or 8 if no constraints were imposed on the choice of the L and ν coefficients. However, these curves should share common parameters determined by the experiments. For example, L_r is the coefficient linking the flow through the proton-pumping cycle (J_r) to the driving reaction affinity of the pump (A_{ch}). A priori, this should not be affected by exchanging NaCl for KCl or treatment of the vesicle membrane with DCCD. Since the background light intensity is constant, L_r should have the same value in each case. For vesicles in KCl or NaCl, pretreatment with DCCD should change L_H^u but not L_K^u or L_{Na}^u. Independent of DCCD pretreatment, changing KCl for NaCl should leave L_H^u unchanged but cause L_K^u to be replaced by L_{Na}^u. Also, changing from KCl to NaCl will mean that the Na^+/H^+ antiporter can function, i.e., L_{ex} is 0 in KCl but L_{ex} is not 0 in NaCl. Therefore, the curves should be fit by such an internally consistent set of parameters. Any differences in the coefficients between curves are determined by the experimental conditions. As shown in Table I and Fig. 7, three of the four curves can be fit under these constraints. However, several empirical modifications had to be assumed to achieve this fitting. These modifications will be discussed in detail.

After turning on the background illumination, there is an ~25 ms period during which there is little or no increase in the membrane potential (Fig. 5). However, the form of Eqs. 6 and 8, implies that if the terms relating to the pumping cycle (L_r and ν_r^H) are held constant vs. time, then $\Delta\Psi$ will begin to increase immediately. The lag period can be modeled based on the following values. L_r is held constant at 3.5×10^{-11} (mol H$^+$)^2/(J · s · g) and ν_r^H at two protons per cycle (Ort and Parson, 1979; Govindjee et al., 1980). However, it is assumed that only those bR molecules cycling through the more slowly decaying M_2 photointermediate pump these protons electrogenically (Kuschmitz and Hess, 1981; Ohno et al., 1983). As shown in Fig. 6, the branching ratio (f) has a strict exponential dependence on the light intensity and hence on the membrane potential. The following equation can be used to estimate the fraction of bR molecules ($f_2 = 1 - f$) cycling through M_2 at any time t

$$f_2(t) = f_2^{min} + (f_2^{max} - f_2^{min})\{1 - \exp[-f_c\Delta\Psi(t)/\Delta\Psi_{max}]\} \quad (9)$$

for $\Delta\Psi_{max} < \Delta\Psi < 0$. f_2^{min} and f_2^{max} are the fractions measured at $\Delta\Psi = 0$ and $\Delta\Psi_{max}$, respectively. f_c is the constant defining the slope of the log (f) vs. steady-state $\Delta\Psi$ (see Fig. 6). For the data shown here, $\Delta\Psi_{max} = -100$ mV, $f_c = 3$, $f_2^{min} = 0.18$, and $f_2^{max} = 0.62$. These values depend on the vesicle preparation. For the data shown in Fig. 7 of reference (Groma et al., 1984), $\Delta\Psi_{max} = -100$ mV, $f_c = 6$, $f_2^{min} = 0.3$, and $f_2^{max} = 0.9$.

The following iterative procedure is then used to obtain the curves shown in Fig. 7. Using the coefficients shown in Table I, starting at $t = 0$ the value of Eqs. 6 or 8 is calculated in 5 ms intervals. Based on the $\Delta\Psi(t)$ value obtained, $f_2(t)$ is calculated and the quantity $[\nu_r^H f_2(t)]$ used in the next interval. In this way the ratio of bR molecules assumed to be pumping electrogenically changes as described by Eq. 9. If a similar procedure is used except that M_1 is assumed to pump, then the potential rises immediately with no lag period. If ν_H is held constant at another value, then changing L_r allows the equations to fit the data. For example: $\nu_r^H = 4$ and $L_r = 2 \times 10^{-10}$ give a reasonably good fit, although not as good as for the values shown in Table I.

There is a pronounced overshoot in $\Delta\Psi$ for vesicles

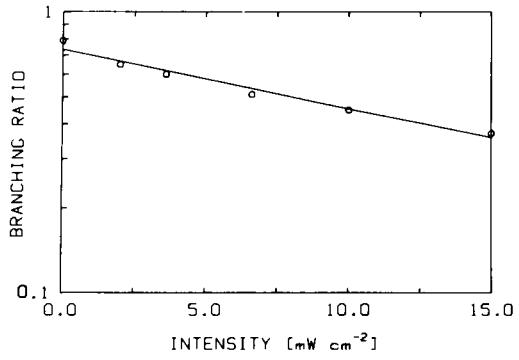

FIGURE 6 Variation of the branching ratio $f = M_1/(M_1 + M_2)$, i.e., the fraction of fast component, with membrane potential in the steady state.

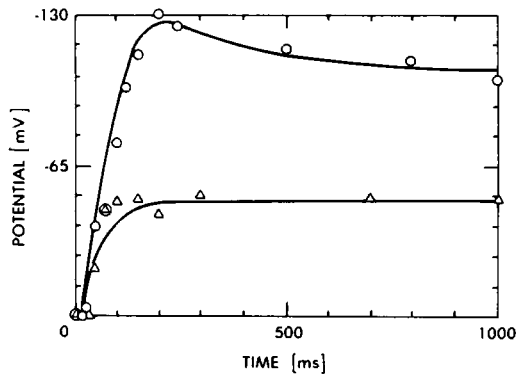

FIGURE 7 Calculated development of the membrane potential (—) based on the $F\Delta\Psi$ equations derived in the text. The values for the L coefficients used to fit the data points (see Fig. 5) are given in Table I. The cell envelope vesicles were loaded and suspended in 3 M NaCl (O) or KCl (Δ) both buffered with 50 mM HEPES (pH 7.5).

suspended in NaCl. Lanyi and Silverman (Lanyi and Silverman, 1979) have reported that sodium/proton antiport in *H. halobium* is a gated function with the threshold at a set value of protonmotive force. Below this pmf the rate of sodium extrusion was negligible but increased linearly with pmf above this gating threshold. For vesicles in KCl (Table I and Fig. 7) the Na^+/H^+ antiporter is inoperative, $L_{ex} = 0$. For vesicles in NaCl with no pH gradient present, it is assumed that each antiporter has the same gating potential $\Delta\Psi_g = -100$ mV. Once this $\Delta\Psi_g$ value is exceeded, any antiporter can be activated and operate at its maximum rate. However, the fraction of the antiporter population (n_{ex}) that is activated at any time (t) depends on a probability function

$$n_{ex}(t) = 1 - 2\frac{\exp[-|\Delta\Psi(t) - \Delta\Psi_g|/\alpha kT]}{1 + \exp[-|\Delta\Psi(t) - \Delta\Psi_g|/\alpha kT]}, \quad (10)$$

where α is a constant and

$$n_{ex}(t) = 0 \text{ for } |\Delta\Psi(t)| < |\Delta\Psi_g|.$$

TABLE I
PHENOMENOLOGICAL COEFFICIENTS FOR THE bR PROTON PUMPING CYCLE (L_r), PASSIVE CATION PERMEABILITIES (L_H, L_K, L_{Na}), AND THE SODIUM/PROTON ANTIPORTER (L_{ex})*

Salt	DCCD	A_{ch}	L_r	L_H^u	L_{cation}^u	L_{ex}
NaCl	(−)	60,000	3.5×10^{-11}	8×10^{-11}	1×10^{-11}	5×10^{-11}
KCl	(−)	60,000	3.5×10^{-11}	2×10^{-10}	2.2×10^{-10}	–0–
KCl	(+)	60,000	3.5×10^{-11}	2×10^{-11}	2.2×10^{-10}	–0–

*See Appendix for definitions and units. The stoichiometries were assumed to be $\nu_r^H = 2$, $\nu_{ex}^H = 2$, and $\nu_{ex}^{Na} = 1$.
‡For comparison between experiments, the value for L_H in NaCl must be multiplied by a correction factor for the increased activity of protons in this salt solution as compared to the same concentration of protons in KCl (see Critchfield and Johnson, 1959). The correction factor is 2.25 for 3 M salt solutions.

This approach is analogous to the Hodgkin and Huxley (1952) description of the gating current for sodium conductance in nerve membranes. No mechanism for gating is proposed here. As above, an iterative calculation is used. After the membrane potential exceeds $\Delta\Psi_g$, the value of $\Delta\Psi(t)$ calculated at 5 ms intervals is used to determine $n_{ex}(t)$. The total number of antiporters is normalized to 1. During the next interval the fraction of additional antiporters to be activated is

$$n_{ex}^{act} = [1 - \Sigma n_{ex}(t)]n_{ex}(t), \quad (11)$$

where the summation is taken from the time when $\Delta\Psi_g$ is exceeded to the previous interval calculated. So the effective coefficient for sodium/proton exchange at time t is taken to be

$$L_{ex}^{act}(t) = \Sigma n_{ex}^{act} L_{ex} \quad (12)$$

for the next calculation (Fig. 7). The adjustable fitting parameter α was set equal to 10.

With these modifications to Eqs. 6 and 8, three of the four curves can be fit using a consistent set of coefficients. The membrane potential data measured for DCCD-pretreated vesicles in NaCl could not be fit by Eq. 8. The $\Delta\Psi$ values for this curve were estimated from a large extrapolation of the calibration curve (Fig. 3 *B*). The linearity shown between $(M_1k_1 + M_2k_2)^{-1}$ and $\Delta\Psi$ may not hold at higher membrane potentials. Also, under these conditions the rise of absorbance change at 418 nm has slowed down significantly. Thus, the measured initial slope of the decay is affected and would tend to overestimate the potential.

DISCUSSION

We have shown that the reciprocal of the initial rate of the overall M decay, $(M_1k_1 + M_2k_2)^{-1}$, linearly correlates with the steady-state $\Delta\Psi$ in *H. halobium* cell envelope vesicles. The kinetic parameters needed to determine this rate can be calculated based on a simplified branched model of the bR photocycle (Groma et al., 1984). Alternatively, the initial linear slope of the overall M decay can be used to measure this rate. Thus, the membrane potential can be estimated with a 2 ms time resolution. Using this technique we have time-resolved the development of $\Delta\Psi$ during illumination of the vesicles. At a constant background light intensity (15 $mWcm^{-2}$), $\Delta\Psi$ rises with a halftime of ~75 ms. The steady-state $\Delta\Psi$ is achieved in ~500 ms and its amplitude is dependent on the cation permeability of the membrane. If CCCP is added to greatly increase the proton permeability, then both the illumination-dependent decrease in the M decay rate and the rise of $\Delta\Psi$ are abolished.

The empirically time-resolved development of $\Delta\Psi$ can be modeled based on equations derived using the thermodynamics of irreversible processes. These equations include terms describing ion fluxes associated with the light-driven

proton pump bacteriorhodopsin, the electrogenic sodium/proton antiporter, and the membrane permeability to cations (H^+, K^+, Na^+). Linear phenomenological coefficients (L) are assumed to link the rate (J) of a given coupled reaction or ionic flux to its driving force (X). The resulting calculations give an internally consistent set of L coefficients in three of the four experimental conditions tested. The calculated L values agree well with estimates of these parameters based on data available in the literature. These results will be discussed in relation to measurements and models presented by other groups.

Westerhoff et al. (1979, 1981) and Hellingwerf et al. (1979) have proposed and tested a description of reconstituted bR liposomes using a similar irreversible thermodynamic formulation. The halftime for the development of $\Delta\Psi$ was estimated to be <1.1 s. A calculation of the $\Delta\Psi$ rise was briefly presented, but the authors noted that the membrane potential-sensitive probes then available responded too slowly to experimentally test the calculated curve. Importantly, a feedback inhibition of the rate of the proton-pumping cycle by the protonmotive force was predicted. Subsequent experiments measured the rate of proton movements in the liposomes vs. the transmembrane proton gradient (ΔpH) (Arents et al., 1981*a*, *b*). This work showed that (*a*) the rates of both the influx and efflux proton flows were linearly dependent on ΔpH up to at least 70 mV and (*b*) the rate of light-driven proton pumping decreased linearly with increasing ΔpH. Westerhoff and Dancshazy (1983) have argued that an inhibition of bR proton pumping by the protonmotive force would result from the faster decaying M-component correlating with the pumping pathway. Our results suggest, but do not prove, that M_2 correlates with pumping (see also Kuschmitz and Hess [1981] and Ohno et al., [1983]). The inhibition of the electrogenic pumping cycle comes instead from the slower M_2 decay kinetics as compared with M_1. Direct measurements of both the kinetics and stoichiometry of any proton movements will be necessary before either model can be verified.

Light-induced membrane potentials in closed membrane systems containing bR have been measured using externally added fluorescent probes and intrinsic carotenoid molecules. The potential-sensitive cyanine dye used by Renthal and Lanyi (1976) in cell envelope vesicles gave steady-state $\Delta\Psi$ values in good agreement with the present results. However, this dye responds to $\Delta\Psi$ by redistributing across the membrane, resulting in a slow response time. Ehrenberg et al. (1984) have used a styryl dye with a response time of <5 μs to measure laser flash-induced potential changes in reconstituted bR liposomes. The reported changes occurred with halftimes of ~40 μs, but no absolute value for the potential was given. Resonance Raman spectroscopy of carotenoid band shifts in intact cells (Szalontai, 1981) and reconstituted bR liposomes (Johnson et al., 1981) indicated potential changes with halftimes of ~80 and ~20 μs, respectively. These rapid changes occur on the same timescale as the initial positive charge displacements measured by the protein electric response signal (PERS) (Keszthelyi and Ormos, 1980). It is possible that a localized electric field could result from charge displacements produced by rapid steps during the proton-pumping cycle (Zimanyi and Garab, 1984). The magnitude of these rapid changes will have to be measured before this can be resolved.

The method used here to measure $\Delta\Psi$ has been calibrated with respect to measured steady-state transmembrane potentials. The results reported measure the true protonmotive force or, more precisely, the difference in the electrochemical potential difference of protons between the two bulk phases. Furthermore, the rate at which $\Delta\Psi$ rises is in good agreement with predictions made on the basis of known, or plausibly estimated, properties of the system (see also Michel and Oesterhelt, 1980). The electrical capacity of the membrane can be assumed to be ~1 $\mu F cm^{-2}$, the area is ~50 $m^2 g^{-1}$, and the rate of electrogenic proton pumping is 2–5 μmol $H^+(g \cdot s)^{-1}$. Thus, the rate of $\Delta\Psi$ generation can hardly exceed 1 $mV ms^{-1}$, which is in agreement with the rate found experimentally.

This rate appears to be very slow when compared with the rate of $\Delta\Psi$ rise reported for other systems. For example, the potential in the thylakoid membrane of chloroplasts can rise to high levels within picoseconds (Junge, 1982). It is likely that the electrical potential measured in chloroplasts is of a different nature from that measured for the present system. If the electrogenic proton pump of the thylakoid membrane is a redox system similar to that proposed by Mitchell in which cycles of electron carriers are linked to hydrogen carriers, then the overall proton-pumping rate is probably limited by the latter process. The movement of electrons along an electron carrier chain may encounter much less resistance than the corresponding proton movements (see Fig. 9 of Junge, 1982). The initiation of a redox pump could induce a rapid movement through electron carriers and hence a redistribution of electrical charges within the membrane. This would give rise to a localized electric field that is sensed by the electrochromic probe used. The rise in the localized electric fields would then be followed by the actual translocation of protons across the membrane. Only cyclic H^+ translocation can produce a true protonmotive force between the two bulk solutions that can ultimately drive coupled processes according to a chemiosmotic mechanism. The initial electrical charge redistribution as sensed by electrochromic probes, albeit an essential step within the overall process, should not be immediately available as a protonmotive force.

In summary, we propose that a localized electric field is different in nature from a delocalized potential as measured here. The inhibition of the bR photocycle, which forms the basis of the present report, is postulated to correlate with a delocalized potential difference. In these experiments <3.5% of the bR molecules are cycling in

response to the background illumination, whereas <0.1% are cycled by the laser probe pulse. The proton-pumping cycle of a single bR molecule does not inhibit its own photocycle, otherwise there would be no intensity dependence of the laser probe pulse (Dancshazy et al., 1983). Thus, the effects we observe must be due to the concerted action of the few background light-driven bR molecules that are cycling incoherently. Both the experiments and the theoretical analysis presented here strongly suggest that the true transmembrane protonmotive force interacts with and inhibits the rate of the electrogenic pumping cycle in bacteriorhodopsin.

We are continuing to test the limits within which these linear nonequilibrium thermodynamic equations can be used to model *H. halobium* bioenergetics. However, the present analysis was first proposed to describe an arbitrary membrane-bound, electrogenic proton pump (Heinz, 1982). This formulation could also be applied to similar problems in other energy-coupling systems. Examples may include the regulation of electron transfer and ATP synthesis in chloroplasts (Graan and Ort, 1983) and the coupling of electron transfer to proton pumping in cytochrome oxidase (Moroney et al., 1984).

APPENDIX

Estimates of the Phenomenological Coupling Coefficients

Preliminary estimates of the parameters used for fitting the time-resolved membrane potential curves with Eqs. 6 and 8 can be made. Here A_{ch}, ν_r^H, and the various L's are calculated from data reported in the literature.

(*a*) A_{ch} is the effective affinity of the pumping reaction cycle. Westerhoff and van Dam (1984) have calculated that photons of 570 nm have a thermodynamic potential of 1.9×10^5 J/mol. Since the quantum efficiency of the bR photoreaction cycle is 0.3 (Becher and Ebrey, 1977), at most 6×10^4 J/mol photons could be converted into useful energy by the bR proton-pumping cycle.

(*b*) ν_r^H is the stoichiometry of protons released per bR photocycle. Values reported range from ~1 H^+ per M photointermediate (Lozier et al., 1976) to ~2 H^+/M (Govindjee et al., 1980) to >3 H^+/M (Kuschmitz and Hess, 1981). We have chosen $\nu_r^H = 2$ but take no position on the absolute value.

(*c*) L_r is the coefficient linking the rate of the proton-pumping cycle to the driving force (Eq. 5b). Hellingwerf et al. (1979) have presented evidence that this parameter depends linearly on both the bR concentration and the light intensity. The cell envelope vesicles used here have ~5 nmol bR/mg protein, the background illumination cycles 3.5% of the bR molecules, and the cycling time is between 20 and 200 ms depending on the M_1/M_2 distribution (Groma et al., 1984). For a lower value (3.5% cycling, 200 ms cycling time)

$$L_r \approx \left(\frac{5 \text{ cycles}}{\text{s}}\right)\left(\frac{1}{6 \times 10^4 \text{J/mol}}\right)\left(\frac{5 \times 10^{-6} \text{mol bR}}{\text{g}}\right)(0.035)$$
$$= 1.5 \times 10^{-11} \frac{\text{mol}^2 \text{ bR cycles}}{\text{J} \cdot \text{s} \cdot \text{g}},$$

while for an upper value (3.5% cycling, 20 ms cycling time)

$$L_r \approx 1.5 \times 10^{-10} \frac{\text{mol}^2 \text{ bR cycles}}{\text{J} \cdot \text{s} \cdot \text{g}}.$$

So, L_r should be between 10^{-11} and 10^{-10} $\text{mol}^2/\text{J} \cdot \text{s} \cdot \text{g}$.

(*d*) L_k^u is potassium leakage coefficient. An approximate value can be calculated based on the initial linear influx of K^+ vs. external KCl concentration (see Figs. 5 and 7 of Lanyi et al., 1979). In this and calculations given below, a membrane potential or protonmotive force of about −120 mV will be assumed for illuminated cell envelope vesicles if no measured value is reported

$$L_K^u \approx \left(2 \times 10^{-6} \frac{\text{mol } K^+}{\text{s} \cdot \text{g} \cdot \text{M}}\right)(3 \text{ M KCl})\left(\frac{1}{-120 \text{ mV}}\right)\left(\frac{-1 \text{ mV}}{96.5 \text{ J/mol}}\right)$$
$$= 5 \times 10^{-10} \frac{\text{mol}^2 K^+}{\text{J} \cdot \text{s} \cdot \text{g}}.$$

Similarly, Cooper et al. (1983) have reported measurements of L_H^u and L_{Na}^u. These values were measured in DCCD-treated vesicles under uncoupled conditions

$$L_H^u \approx 5 \times 10^{-11} \frac{\text{mol}^2 H^+}{\text{J} \cdot \text{g} \cdot \text{s}}$$

and

$$L_{Na}^u \approx 1 \times 10^{-10} \frac{\text{mol}^2 Na^+}{\text{J} \cdot \text{g} \cdot \text{s}}.$$

Schobert and Lanyi (see Fig. 11 of Schobert and Lanyi, 1982) found an extrusion of 0.04 M Cl^- in 20 min of illumination for bR-containing cell envelope vesicles. This gives

$$L_{Cl}^u \approx 1 \times 10^{-11} \frac{\text{mol}^2 Cl^-}{\text{J} \cdot \text{g} \cdot \text{s}}$$

and justifies the assumption that ions other than H^+, K^+, and Na^+ need not be considered.

(*e*) L_{ex} is the rate coefficient for the Na^+/H^+ antiporter (Eq. 7c). Values can be calculated from several reports and show a large variability. This may be due to the difficulties inherent in measuring sodium fluxes. Eisenbach et al. (see Table I of Eisenbach et al., 1977) measured active sodium extrusion from cell envelope vesicles and found that DCCD had no inhibitory effects. Their results would suggest

$$L_{ex} \approx 2 \times 10^{-10} \frac{\text{mol}^2 Na^+}{\text{J} \cdot \text{g} \cdot \text{s}}$$

for an illumination intensity of 80 mWcm^{-2}.

Lanyi and MacDonald (1976) (see Figs. 1 and 2*A* of Lanyi and Silverman, 1979) also found active sodium extrusion. The Na^+ efflux rate was sensitive to both the light intensity and the protonmotive force. For pmf lower than −150 mV of which the $\Delta\Psi$ component was less than −120 mV, Na^+ efflux was negligible. Above these values, it can be estimated that

$$L_{ex} \approx 2.5 \times 10^{-9} \frac{\text{mol}^2 Na^+}{\text{J} \cdot \text{s} \cdot \text{g}}.$$

However, above this gating threshold the Na^+ pumping rate appears to correlate with the illumination intensity, i.e., bR proton-pumping rate, not with the pmf. This follows from the near saturation of pmf at 25 to 40 mWcm^{-2} (Groma et al., 1984; Renthal and Lanyi 1976), while Na^+ efflux rates continue to increase with illumination up to 200 mWcm^{-2} (Lanyi and Silverman, 1979).

Cooper et al. (1983) used H^+ movements driven by artificial sodium gradients (<0.1 pNa units) to measure

$$L_{ex} \approx 1 \times 10^{-11} \frac{\text{mol}^2 Na^+}{\text{J} \cdot \text{g} \cdot \text{s}}.$$

These measurements were done using DCCD-treated cell envelope vesicles with $\Delta\Psi$ held to zero by a high $TPMP^+$ concentration. Thus, this value may be the exchange rate through the antiporter below the gating potential.

Thanks are due to Drs. P. C. Mowery, Zs. Dancshazy, and G. Groma for their helpful discussions concerning this work. This research was supported by the National Institutes of Health (NIH) Program Project Grant GM-27057, National Aeronautics and Space Administration (NASA) grant NSG-7151, and NIH Grant GM-26554.

Received for publication 20 November 1984 and in final form 4 June 1985.

REFERENCES

Arents, J. C., K. J. Hellingwerf, K. van Dam, and H. V. Westerhoff. 1981*a*. Bacteriorhodopsin in liposomes: Quantitative evaluation of deltapH changes induced by variations of light intensity and conductivity parameters. *J. Membr. Biol.* 60:95–104.

Arents, J. C., H. van Dekken, K. J. Hellingwerf, and H. V. Westerhoff. 1981*b*. Linear relations between proton current and pH gradient in bacteriorhodopsin liposomes. *Biochemistry.* 20:5114–5123.

Becher, B., and T. G. Ebrey. 1977. The quantum efficiency for the photochemical conversion of the purple membrane protein. *Biophys. J.* 17:185–191.

Cooper, S., I. Michaeli, and S. R. Caplan. 1983. Characterization of sodium and proton flows in sub-bacterial particles of *Halobacterium halobium* in terms of nonequilibrium thermodynamics. *Biochim. Biophys. Acta.* 736:11–27.

Critchfield, F. E., and J. B. Johnson. 1959. Effect on neutral salts on the pH of acid solutions. *Anal. Chem.* 31:570–572.

Dancshazy, Zs., S. L. Helgerson, and W. Stoeckenius. 1983. Coupling between the bacteriorhodopsin photocycle kinetics and the protonmotive force. I. Single flash measurements in *Halobacterium halobium* cells. *Photobiochem. Photobiophys.* 5:347–357.

Eisenbach, M., S. Cooper, H. Garty, R. Johnstone, H. Rottenberg, and S. R. Caplan. 1977. Light-driven sodium transport in sub-bacterial particles of *Halobacterium halobium. Biochim. Biophys. Acta.* 465:599–613.

Ehrenberg, B., F. Meiri, and L. M. Loew. 1984. A microsecond kinetic study of the photogenerated membrane potential of bacteriorhodopsin with a fast responding dye. *Photochem. Photobiol.* 39:199–205.

Govindjee, R., T. G. Ebrey, and A. R. Crofts. 1980. The quantum efficiency of proton pumping by the purple membrane of *Halobacterium halobium. Biophys. J.* 30:231–242.

Graan, T., and D. R. Ort. 1983. Initial events in the regulation of electron transfer in chloroplasts. The role of the membrane potential. *J. Biol. Chem.* 258:2831–2836.

Groma, G. I., S. L. Helgerson, P. K. Wolber, D. Beece, Zs. Dancshazy, L. Keszthelyi, and W. Stoeckenius. 1984. Coupling between the bacteriorhodopsin photocycle and the protonmotive force in *Halobacterium halobium* cell envelope vesicles. II. Quantitation and preliminary modeling of the M → bR reactions. *Biophys. J.* 45:985–992.

Heinz, E. 1980. Electrogenic and electrically silent proton pumps. *In* Hydrogen Ion Transport in Epithelia. I. Schulz, G. Sachs, J. G. Forte, and K. J. Ullrich, editors. Elsevier/North-Holland Press, Amsterdam. 41–45.

Heinz, E. 1982. Response of the protonmotive force to the pulse of an electrogenic pump. *Curr. Top. Membr. Transp.* 16:249–256.

Helgerson, S. L., C. Requadt, and W. Stoeckenius. 1983. *Halobacterium halobium* photophosphorylation: Illumination-dependent increase in the adenylate energy charge and phosphorylation potential. *Biochemistry.* 22:5746–5753.

Hellingwerf, K. J., J. C. Arents, B. J. Scholte, H. V. Westerhoff. 1979. Bacteriorhodopsin in liposomes II. Experimental evidence in support of a model system. *Biochim. Biophys. Acta.* 547:561–582.

Hodgkin, A. L., and A. F. Huxley. 1952. A quantitative description of membrane current and its application to conduction and excitation in nerve. *J. Physiol. (Lond.).* 117:500–514.

Jap, B. K., and R. M. Glaeser. 1983. Dicyclohexylcarbodiimide inhibits proton transport in bacteriorhodopsin. *Biophys. J.* 41(2, Pt.2):334*a*. (Abstr.)

Johnson, J. H., A. Lewis, and G. Gogel. 1981. Kinetic resonance Raman spectroscopy of carotenoids: A sensitive kinetic monitor of bacteriorhodopsin mediated membrane potential changes. *Biochem. Biophys. Res. Commun.* 103:182–188.

Junge, W. 1982. Electric generators in photosynthesis. *Curr. Top. Membr. Transp.* 16:431–465.

Keszthelyi, L., and P. Ormos. 1980. Electrical signals associated with the photocycle of bacteriorhodopsin. *FEBS (Fed. Eur. Biochem. Soc.) Lett.* 109:189–193.

Kuschmitz, D., and B. Hess. 1981. On the ratio of the proton and photochemical cycle in bacteriorhodopsin. *Biochemistry.* 20:5950–5957.

Lanyi, J. K. 1972. Studies of the electron transport chain of extremely halophilic bacteria. VII. Solubilization properties of menadione reductase. *J. Biol. Chem.* 247:3001–3007.

Lanyi, J. K., and R. E. MacDonald. 1976. Existence of electrogenic H^+/Na^+ antiport in *Halobacterium halobium* cell envelope vesicles. *Biochemistry.* 15:4608–4614.

Lanyi, J. K., and M. P. Silverman. 1979. Gated transport functions in *Halobacterium halobium. J. Biol. Chem.* 254:4750–4755.

Lanyi, J. K., S. L. Helgerson, and M. P. Silverman. 1979. Relationship between protonmotive force and potassium ion transport in *Halobacterium halobium* envelope vesicles. *Arch. Biochem. Biophys.* 193:329–339.

Lozier, R. H., W. Niederberger, R. A. Bogomolni, S. B. Hwang, and W. Stoeckenius. 1976. Kinetics and stoichiometry of light-induced proton release and uptake from purple membrane fragments, *Halobacterium halobium* cell envelopes, and phospholipid vesicles containing oriented purple membrane. *Biochim. Biophys. Acta.* 440:545–556.

Michel, H., and D. Oesterhelt. 1980. Electrochemical proton gradient across the cell membrane of *Halobacterium halobium.* Effect of *N,N'*-dicyclohexylcarbodiimide, relation to intracellular ATP-, ADP- and phosphate concentrations and the influence of the potassium gradient. *Biochemistry.* 19:4607–4614.

Mitchell, P. 1968. Chemiosmotic Coupling and Energy Transduction. Glynn Research Ltd., Bodmin, England.

Moroney, P. M., T. A. Schole, and P. C. Hinkle. 1984. Effect of membrane potential and pH gradient on electron transfer in cytochrome oxidase. *Biochemistry.* 23:4991–4997.

Ohno, K., R. Govindjee, and T. G. Ebrey. 1983. Blue light effect on proton pumping by bacteriorhodopsin. *Biophys. J.* 43:251–254.

Ort, D. R., and W. W. Parson. 1979. The quantum yield of flash-induced proton release by bacteriorhodopsin-containing membrane fragments. *Biophys. J.* 25:341–353.

Renthal, R., and J. K. Lanyi. 1976. Light-induced membrane potential and pH gradient in *Halobacterium halobium* envelope vesicles. *Biochemistry.* 15:2136–2143.

Schobert, B., and J. K. Lanyi. 1982. Halorhodopsin is a light driven chloride pump. *J. Biol. Chem.* 257:10306–10313.

Stoeckenius, W., R. H. Lozier, R. A. Bogomolni. 1979. Bacteriorhodopsin and the purple membrane of *Halobacteria. Biochim. Biophys. Acta.* 505:215–278.

Stoeckenius, W., and R. A. Bogomolni. 1982. Bacteriorhodopsin and related pigments in *Halobacteria. Annu. Rev. Biochem.* 52:587–615.

Szalontai, B. 1981. Light-induced membrane potential changes in *Halobacterium halobium* observed with high time resolution by resonance Raman spectroscopy. *Biochem. Biophys. Res. Commun.* 100:1126–1130.

Westerhoff, H. V., B. J. Scholte, and K. J. Hellingwerf. 1979. Bacteriorhodopsin in liposomes. I. A description using irreversible thermodynamics. *Biochim. Biophys. Acta.* 547:544–560.

Westerhoff, H. V., K. J. Hellingwerf, J. C. Arents, B. J. Scholte, K. van Dam. 1981. Mosaic nonequilibrium thermodynamics describes biological energy transduction. *Proc. Natl. Acad. Sci.* USA. 78:3554–3558.

Westerhoff, H. V., B. A. Melandri, G. Venturoli, G. F. Azzone, and D. B. Kell. 1984. Mosaic protonic coupling hypothesis for free energy transduction. *FEBS (Fed. Eur. Biochem. Soc.) Lett.* 165:1–5.

Westerhoff, H. V., and Zs. Dancshazy. 1984. Keeping a light-driven proton pump under control. *Trends Biochem. Sci.* 9:112–117.

Westerhoff, H. V., and K. van Dam. 1984. Mosaic Non-Equilibrium Thermodynamics and (Control of) Bioenergetics. Elsevier Scientific Publishing Co., Amsterdam.

Zimanyi, L., and Gy. Garab. 1984. Calculation of the electric potential and the ion concentration distribution due to charge separation in a closed membrane vesicle. *Third Eur. Bioenerg. Conf.*, Sept. 2–7, Hannover, Federal Republic of Germany. 281–282.